The Heat Transfer and Fluid Flow Investigations of Single Dimple with Straight and Curved Arch Turbulator within in a Duct

Sandeep Sadashiv Kore[1,*], Manoj Kumar Chaudhary[2], Parimal Sharad Bhambare[3], Dinesh Keloth Kaithari[3]

1   Department of Mechanical Engineering, Vishwakarma Institute of Information Technology, Pune, Maharashtra 411048, India
2   Department of Mechanical Engineering, Trinity Academy of Engineering, Pune, Maharashtra 411048, India
3   Department of Mechanical Engineering, College of Engineering, National University of Science and Technology, Muscat, Oman

ARTICLE INFO	ABSTRACT
Article history: Received 23 October 2023 Received in revised form 18 February 2024 Accepted 29 February 2024 Available online 15 March 2024 *Keywords:* Heat transfer enhancement; duct flow; vortex generation; dimple surface; forced convection	An experimental study was conducted to examine the impact of a single dimple with an arch-type turbulator on heat transfer and fluid friction. The square duct has a 4:1 aspect ratio. Reynolds numbers range from 10,000 to 35,000 depending on hydraulic diameter, maintaining as 0.5 aspect ratio between duct height and dimple diameter. Dimple depth to print diameter ratio is 0.3, which is maintained constant. Two different types of arch turbulators are tested in the first half of the dimple to improve the fluid velocities and heat transfer. The turbulators used in the investigations are both curved and straight type. Curved arch turbulators included angles are 45°, 60°, or 90°, whereas straight arch turbulators are inclined to the surface at a 12° angle. At the dimple's leading edge, an arch turbulator is installed. The experimental findings are displayed as Nusselt number, normalized Nusselt number, friction factor, normalized friction factor, and thermal performance. According to the experimental findings, turbulators with a 60° curved arch operate better than those with 45° and 90° curved arches. Compared to all other arch turbulators, the straight arch turbulator achieves the highest thermal performance.

1. Introduction

Passive methods, such as different types of ribs, can be used to increase the rate of heat transfer inside the duct like dimpled surface and pin fins. These techniques are used for combustion chamber liners, internal cooling of turbine blades, solar air heaters, electronic cooing devices, medical equipment's and industrial heat exchangers. Now days dimpled surfaces are used cause of considerable heat transfer rate at lesser pressure penalty. Along with dimpled surface some compound techniques are also tried to improve heat transfer rate. Available literature provides data about effect of different dimple parameters.

Russian aerodynamic society utilizes dimpled surface for reduction of drag as well as heat transfer enhancement. They employ regular arrays of dimpled surface, staggered array of dimpled surface in

annular passage, flow through converging and diverging dimple and flow through narrow duct with spherical dimples placed on two opposite walls with change in relative position [1-4]. Heat transfer enhancement of 150 percent compared to flat plates is reported sometimes with lesser pressure penalty [5]. Another recent study demonstrates that over a range of Reynolds numbers, a 2.5-fold increase in the rate of heat transfer is observed in comparison to a smooth plate. The pressure penalty is roughly half of what is produced by various types of rib turbulators.

According to Moon *et al.,* [6], the pressure penalty and increase in heat transfer rate are roughly consistent over a wide range of Reynolds numbers and duct heights. Mahmood *et al.,* [7] identified the mechanisms underlying local and regionally averaged heat transfer enhancement on plain duct surfaces with an array of dimples on one wall.

Isaev *et al.,* [8] considered the heat transfer and fluid flow in a single spherical dimple. He described the internal flow pattern of the dimple. Ligrani *et al.,* [3,9] investigated the effects of dimple depth on vortex shape and surface heat transfer, as well as the impacts of relative dimple and protrusion position on opposing duct walls. Depth of dimple influence on a surfaces local environment aspect ratio, and flow structure all acting together, Nusselt number distributions, Nusselt number distributions alone, and flow structure resulting from dimple depressions on a channel surface [2,3,7]. Patil *et al.,* [10] and Yadav *et al.,* [11] investigated heat exchanger tube for different flow blockages with wall attached circular ring turbulator and twisted tape with Fe_3O_4 nanofluid.

Researchers are investigating the techniques like jet impingement cooling in a heat exchanger, twisted tape inserts and circular ring turbulator for heat exchanger tube heat transfer enhancement [12-14].

The present investigation is based on heat transfer enhancement from single dimple with arch and straight type of turbulator. The ratio of dimple depth to dimple print diameter 'δ/D' is 0.3, kept constant. The curved and straight arch turbulator is kept at leading edge of the dimple. The experimental results are presented for different arch turbulator with included angle 45 °, 60 °and 90° for curved and 12 ° for straight turbulator. The Re_{Dh} based on hydraulic diameter is varied from 10,000 to 35,000. Data on average Nusselt number, normalized Nusselt number, friction factor, normalized friction factor, and thermal performance are reported in this study.

2. Experimental Investigations
2.1 Experimental Set Up

In order to research the impact of a dimple with an arch turbulator on heat transfer and fluid attribute in a rectangular duct, an experimental facility has been designed and produced. The experimental facility's schematic layout is depicted in Figure 1(a).

The setup is an open system type. The following elements are linked on the blower's suction side; the setup is an open system type. 1) Development section, 2) Test section, 3) The exit section with the mixing chamber, 4) A flow measuring instrument (orifice), 5) A micro manometer (LC=1Pascal) for gauging pressure drops over the test duct.

The dimpled surface is formed within the aluminium block by CNC machining. The print diameter of the dimple is 50 mm while dimple depth is 15mm kept constant through the experiment. The exit and entry lengths of the test facility are 250 mm (6.25Dh) and 1000 mm (25Dh) respectively. The exit section is of 250mm consisting of mixing chamber. The mixing chamber is used after the test section for proper mixing of hot and cold air and to minimize the end effects. During the experimentation constant heat flux boundary condition is imposed, while inlet velocity of the air is changing with respect to Reynolds number. To provide uniform heat flux boundary condition of 7500W/m^2,

cylindrical electric heaters of size 10 mm x 12 mm are used. The heaters are located below the dimpled surface. The test plate is housed in Bakelite box of size 160 x 160 x 12 mm and is clamped to test air duct. In order to minimize heat losses from all directions glass wool insulation is used. The test plate is insulated from all four sides by glass wool insulation of 25 mm thick. The bottom of the test section is insulated by 6mm asbestos sheet followed by 40 mm glass wool insulation. An orifice meter is used to measure mass flow rate of air. For adjusting the flow rate, a flow control valve is provided in the line with duct. The surface temperature is measured with 14 calibrated k-type thermocouples (24 SWG). For measuring inlet air temperature two thermocouples are used and for exit air temperature three thermocouples are used. The locations of thermocouples on the test plate are shown in Figure 1(b). The thermocouple emf is measured by mili-voltmeter. A differential micro-manometer of least counts 0.1WC is used to measure the pressure drop across the duct.
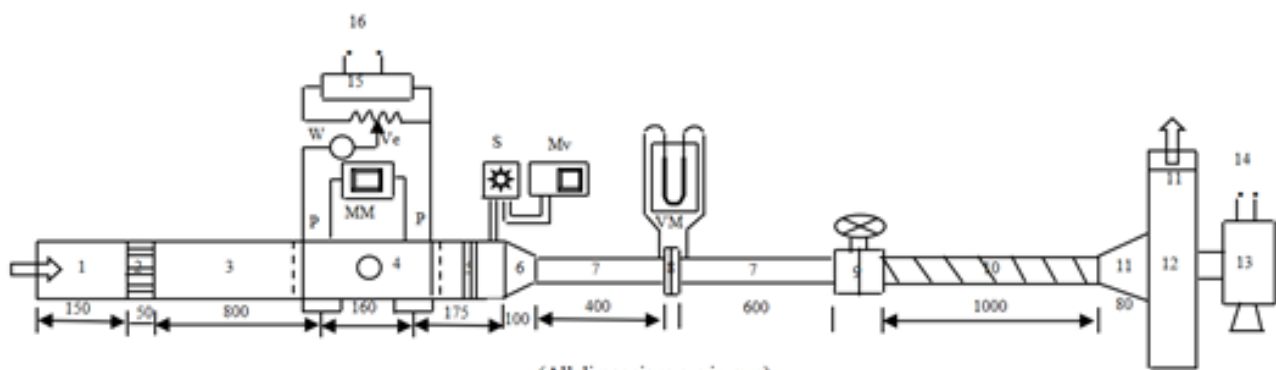
(All dimensions are in mm)

1. Inlet section	7. Rigid pipe	13. 2hp, 2880 rpm motor	Mv. Milli voltmeter
2. Honeycomb section	8. Orifice meter	14. 3φ, 440V powers supply	S. Selector switch
3. Development section	9. Control valve	15. Servo stabilizer	W. Watt meter
4. Test section	10. Flexible hose	16.1φ, 230V power supply	Ve. Variac
5. Outlet section	11. Pressure reducer	VM. Vertical manometer	P. Pressure taps
6. Transition piece	12. Centrifugal blower	MM. Micro manometer	

(a)
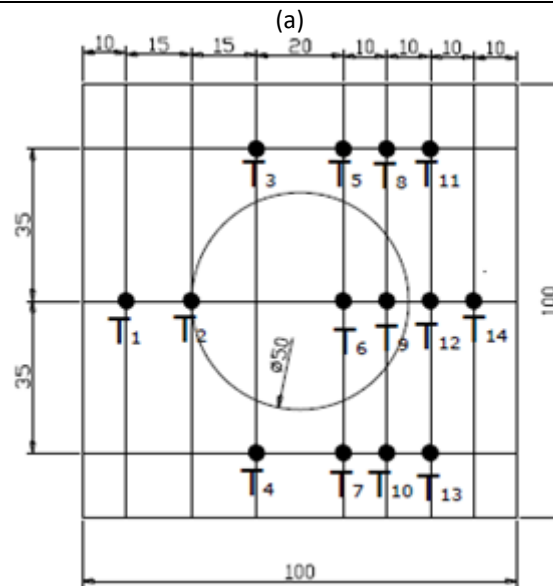
(All dimensions are in mm)

(b)

Fig. 1. (a) Schematic diagram of experimental set up, (b) Locations of thermocouples

2.2 Flow Structure Due to Dimple Surface

In the present investigations dimple surface of print diameter 50 mm and depth 15 mm is used. For the flow simulation Ansys Fluent was used. The numerical formulation and boundary conditions are used as per Suhas [15]. The velocity inlet boundary condition is employed at the inlet of the duct. At the duct outlet pressure out let (atmospheric pressure) boundary condition is employed. The constant heat flux boundary condition is employed at the bottom of the duct based on projected area. The flow structure and temperature field due to dimple surface is presented in Figure 2.
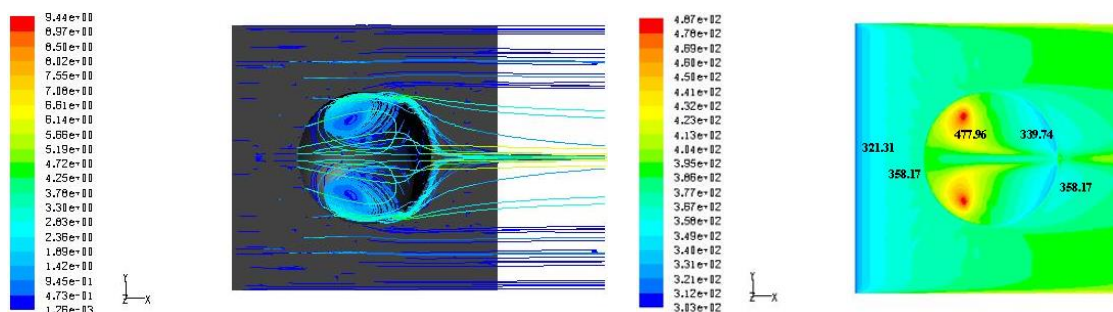
Fig. 2. Flow structure and temperature field due to dimple surface

It is observed from Figure 2, if the fluid enters inside the dimple there is sudden enlargement due to which velocity of the fluid decreases and flow reverse in backward direction. It is shown in Figure 2 two symmetric vortices are formed within the dimple. These vortices cause jetting of the fluid because inside the dimple pressure is high compared to outside. These vortices impinge on the trailing edge of the dimple which is clearly shown in Figure 2. These vortices develop high heat zone. It is observed in the temperature profile where vortices are formed there temperature is higher. The Figure 3(a), indicates variation of 'u' velocity within dimple surface at mid and trailing plane. It is observed that within dimple at the bottom normalized 'u' velocity is lower due to formation of vortices. It is going to increase at the center of the dimple. At the trailing edge of the dimple also we observe variation of normalized 'u' velocity due to ejection of the fluid.

Figure 3(b) indicates variation of 'w' velocity at the mid plane and trailing edge of the dimple. It is seen that positive and negative component of 'w' velocity is observed within dimple. Which shows flow is moving in downward and upward direction. This is due to formation of vortices and ejection of the fluid from the dimple. Figure 3(c) indicates the velocity gradient and shear stress at the symmetry plane of the dimple surface. It is seen that these is sudden drop of velocity gradient and shear stress at the leading edge of the dimple due to sudden expansion of the fluid. The gradually velocity gradient and shear stress increases and become maximum at the trailing edge.
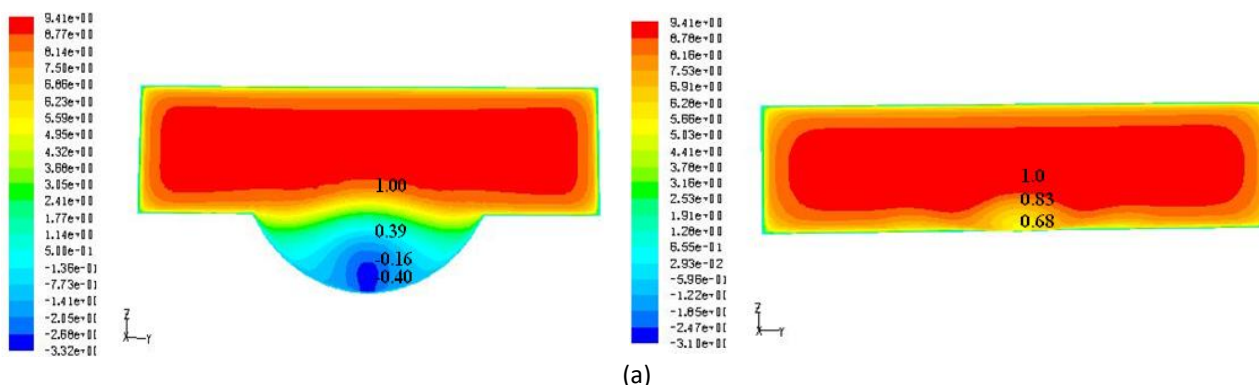
(a)
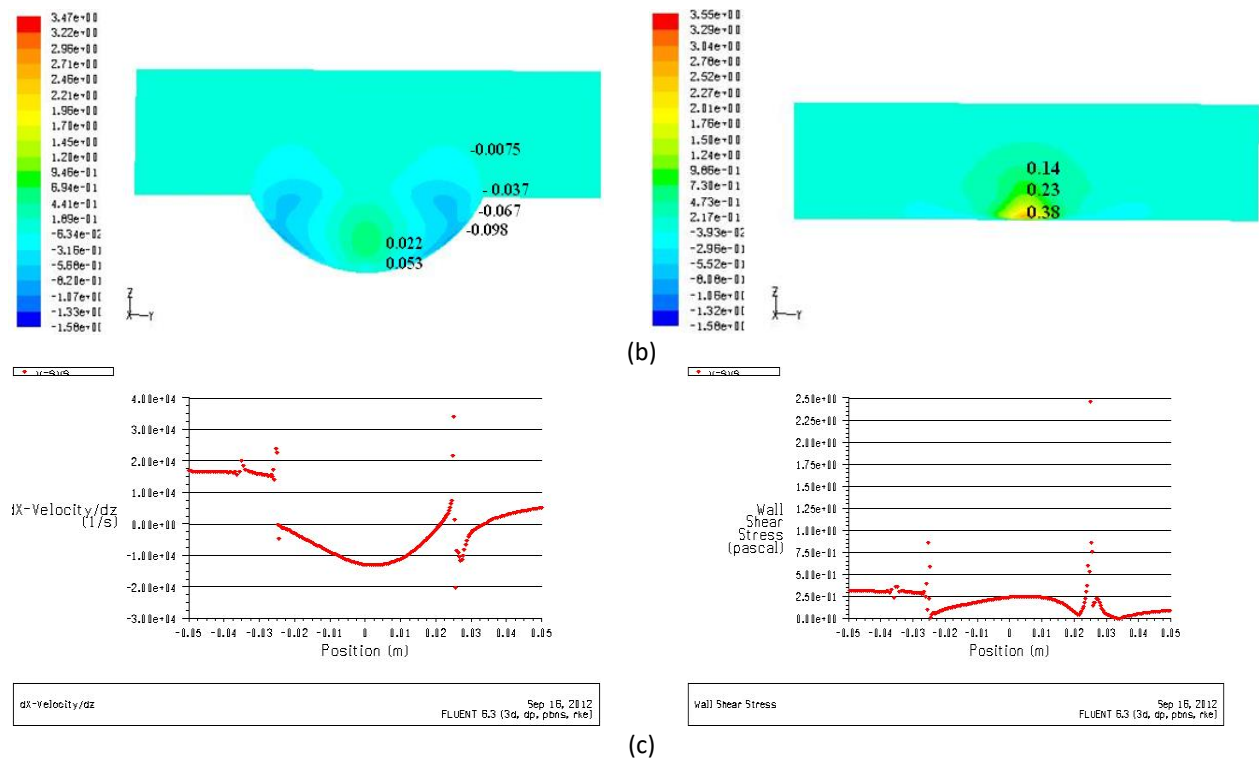
Fig. 3. (a) U velocity due to dimple at mid plane and trailing plane, (b) W velocity due to dimple at mid plane and trailing plane, (c) Velocity gradient and shear stress at the plane centre plane

Due to formation of low velocity and high temperature zone at the leading edge of the dimple, an arch and straight type of turbulator is designed. The purpose of using arch and straight type of turbulator is to increase the localized velocity within initial part of the dimple. In the following section details of the turbulator are discussed.

2.3 Turbulator Geometry

An arch and straight turbulator is developed to break the viscous sub layer in number of ways. The straight arch turbulator is manufactured from thin aluminum sheet of 0.5 mm thickness and placed at leading edge of the dimple. The curved arch turbulator is made from aluminum pipe that is 2 mm thick, has an inner radius of 50 mm, and a turbulator height of 3.5 mm. There are three different total inclusive curved arch angles: 45°, 60°, and 90°. Aluminum glue is used to affix the turbulators to the base plate. Both turbulators are intended to shear or break viscous flow and accelerate flow in the first half of the dimple when fluid velocity is lower. Figure 4 shows details of curved arch turbulator.

Figure 5(a) shows the details of straight arch turbulator. The height of the straight arch turbulator is 12 mm, while open passage below the turbulator is 1.5 mm. Its top and bottom curved edge breaks the shear layer. The two side legs cause also cause mixing of primary and secondary flow. Figure 5(b) shows plausible flow structure. The bottom and top horizontal edge of straight arch turbulator breaks the viscous layer by two ways. The horizontal edge (open passage) may force the flow inside the dimple with higher intensity and more reattachment points. The two legs of the turbulator break the boundary layer by four ways casing mixing of the primary and secondary flow.
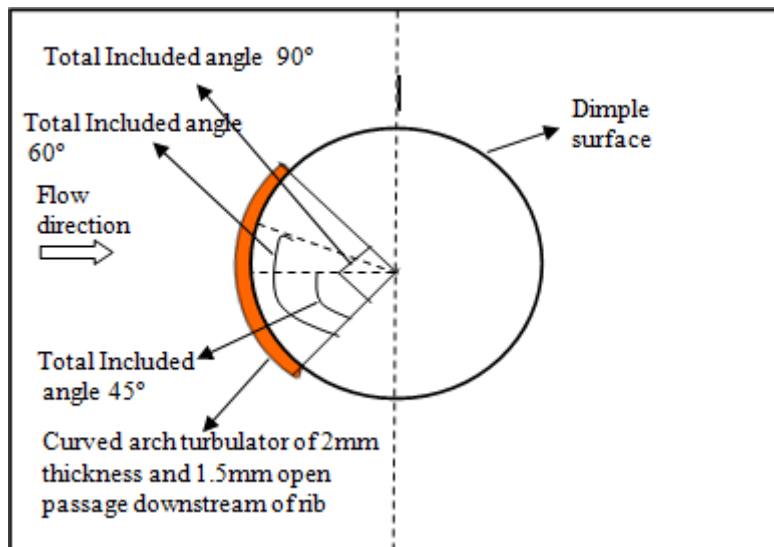
Fig. 4. Details of curved arch turbulator placed on test plate
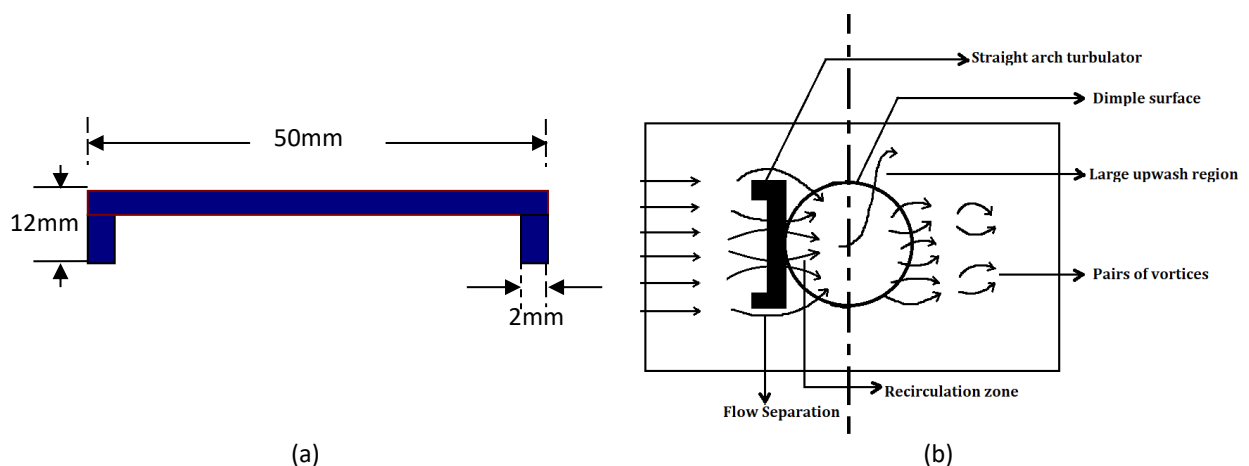
Fig. 5. (a) Details of straight arch turbulator geometry, (b) Plausible flow structure due to straight arch turbulator

The following correlations are developed using excel programming used to find out heat loss from the test section shown by Eq. (1). The heat utilized to change the enthalpy of air is find out by subtracting loss from heater input supplied. To measure the heat loss eight thermocouples from all the four sides are placed.

$$Q_l = 0.687 \, (T_{bs}-T_{ai}) + 0.08 \times 10^{-4} \, (T_{bs}-T_{ai})^2 \tag{1}$$

3. Results and Discussion
3.1 Validation Test for Smooth Duct

The test set up is validated with available equations from the literature. For the heat transfer Gnielinski and Dittus-Boelter equation are used while for friction factor modified Blasius equation is used. The Nusselt number obtained from smooth plate is used to normalize the Nusselt number obtained from dimpled plate. Figure 6 shows comparison of Nusselt number obtained from experimental results and available correlations for smooth plate. The predicted values of Nusselt number are given by Eq. (2).
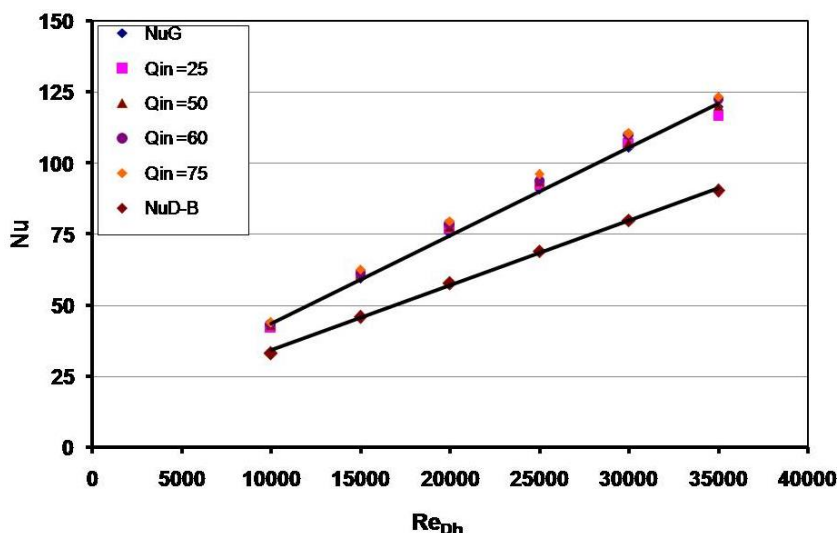
Fig. 6. Baseline Nusselt No. for smooth plate

$$Nu = 0.0214(Re_{Dh}^{0.8} - 100) \, Pr^{0.4} \, [1 + (Dh/L)^{2/3}] \text{ and } Nu = 0.023 \, Re^{0.8} \, Pr^{0.4} \tag{2}$$

It can be seen from the graph that experimental data agrees with Gnielinski equation with maximum deviation of +6% and -3 %. A friction factor characteristic of smooth plate is compared with modified Blasius equation given by Eq. (3).

$$f = 0.085 \, Re^{-0.25} \tag{3}$$

From Figure 7, it is observed that variation of friction factor for smooth plate with modified Blasius equation is within 7% compared to experimental results. The experimental friction factor of smooth plate is used to normalize the friction factor obtained from dimpled surfaces.
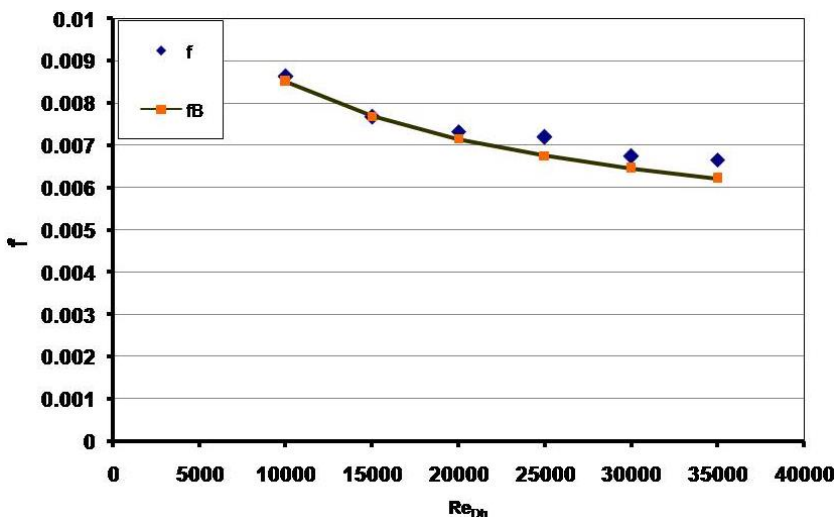
Fig. 7. Baseline friction factor for smooth plate

3.2 Effect of Arch Turbulator on Nu and Nu/Nu$_0$

The Nu and Nu/Nu$_0$ rise with an increase in Re$_{Dh}$ for all geometries, as seen in Figure 8 and Figure 9, is as expected. For all arch turbulators, the rise in Nu and Nu/Nu$_0$ is greater than for dimple geometry with δ/D=0.3. Straight arch turbulators have bigger increases in Nu and Nu/Nu$_0$ than all

other types of turbulators at all Re_{Dh}. In comparison to the 45° and 90° curved arch turbulators, the 60° curved arch turbulator exhibits higher Nu and Nu/Nu_0. The rise in flow velocities inside the leading portion of the dimple is what causes the heat transfer rate for the 60° curved arch turbulator to increase. The 60° curved arch turbulator may forces larger volume of fluid with increased velocity inside the dimple. Compared to other curved arch turbulator geometries, this increases the rate of heat transfer. The flow may be diverted away from the dimple by the 45° curved arch turbulators legs, which results in a slower rate of heat transfer. The turbulator legs' ability to shear the boundary layer may be decreased in the case of turbulators with 90° arches. The increase in heat transfer rate caused by turbulators with straight, 45°, 60°, and 90° curved arches are 2.12, 1.8, 1.96, and 1.83 times flat plate, respectively.
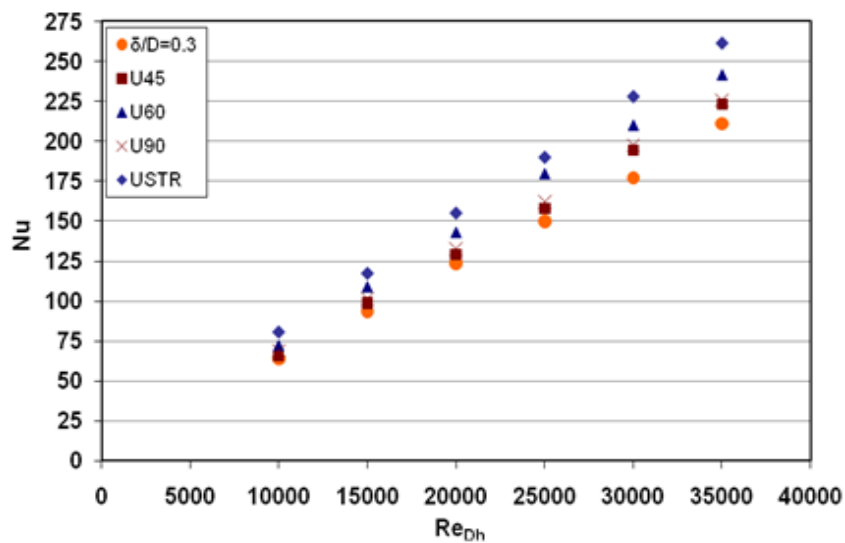
Fig. 8. Nu as a function of Re_{Dh} for different arch turbulator
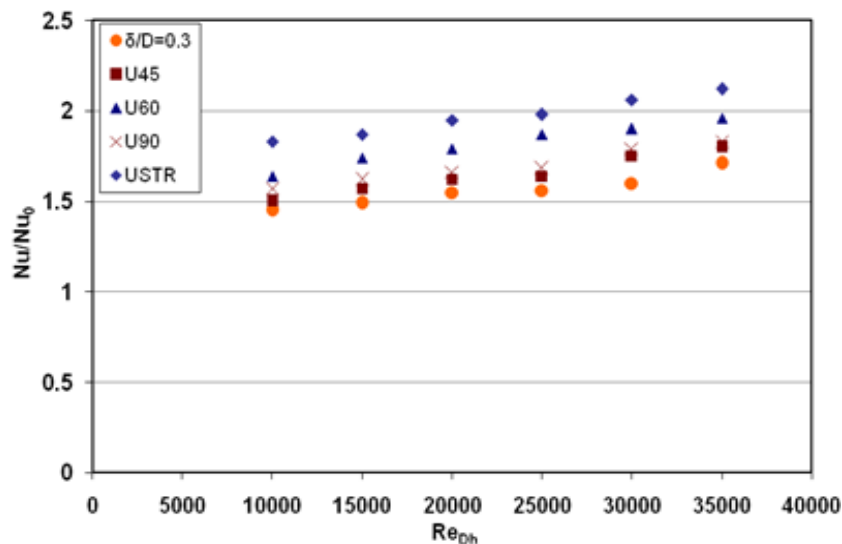
Fig. 9. Nu/Nu_0 as a function of Re_{Dh} for different arch turbulator

3.3 Effect of Arch Turbulator on f and f/f_0

Figure 10 and Figure 11 depict how the straight and curved arch turbulators affect fluid friction. As Re_{Dh} rises, all of the arch turbulators as depicted in Figure 8 experience expected friction factor decreases. This can be because the viscous sublayer is suppressed. For 45° curved arch turbulators,

the 'f' and 'f/f0' are at their lowest values. The 'f' and f/f0' are higher for 90° curved arch turbulators than for other curved arch turbulators. This is because, in comparison to other curved arch turbulators, 90° curved turbulators occupy a longer curved length or restrict a larger flow area. The 'f' and 'f/f0' for the straight arch turbulator are between the 60° and 90° curved arch turbulator. In comparison to 60° and 90° curved arch turbulators, the straight arch offers less flow resistance because it is angled at 12° to the flat surface at the entry of the dimple.
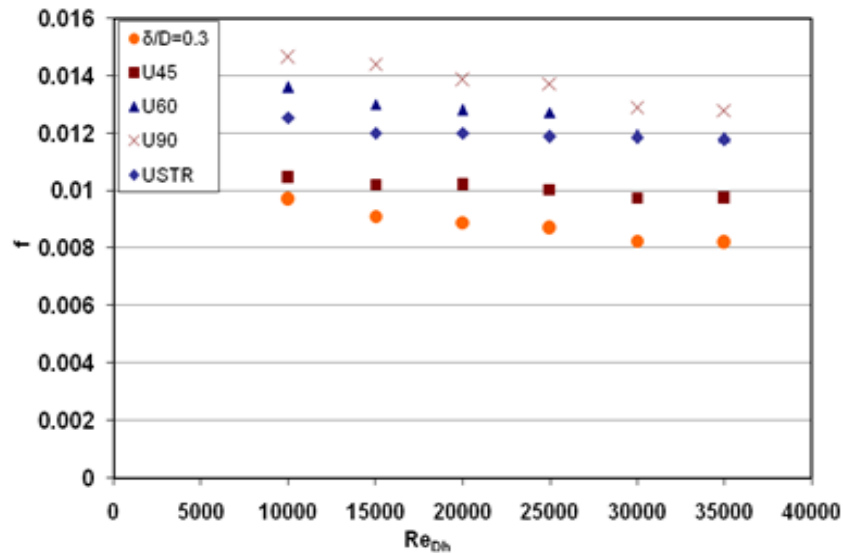
Fig. 10. f as a function of Re_{Dh} for different arch turbulator
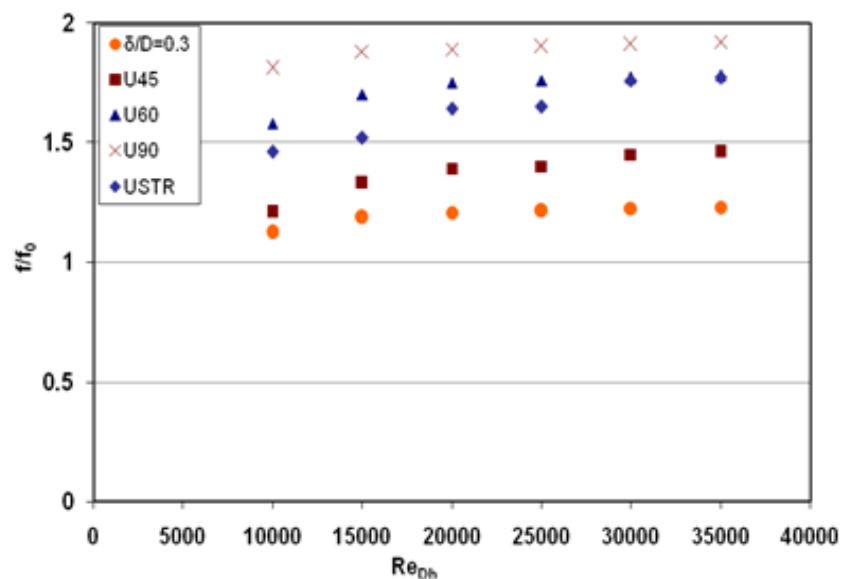
Fig. 11. f/f_0 as a function of Re_{Dh} for different arch turbulator

3.4 Effect of Arch Turbulator on η_{th}

Figure 12 compares the thermal performance of all arch turbulator configurations with dimple depth δ/D=0.3 and all other variants. The thermal performance factor is found out using

$$\eta_{th} = \frac{\left[\dfrac{Nu}{Nu_0}\right]}{\left[\dfrac{f}{f_0}\right]^{\frac{1}{3}}}$$

(4)

Given that it offers more flow resistance, the 90° curved arch turbulator performs thermally less well than one with a dimple depth of $\delta/D=0.3$. It also changes the direction of the fluid flow to avoid the indentation. As a result, the amount of fluid entering the dimple and ejecting from the dimple is reduced. In comparison to dimple depth $\delta/D=0.3$, the thermal performance of curved arch turbulators at 45°, 60°, and straight angles is higher. Straight arch turbulators provide the maximum thermal performance when compared to curved ones. The maximum thermal performance values are 1.75 for a straight arch turbulator and 1.59, 1.62, and 1.47 for curved arch turbulators at angles of 45, 60, and 90. The uncertainty in the measurement is calculated using method suggested by Kline and McClintock [16] and error in measurement is considered using Miller [17]. The uncertainty in the calculation of Re_{Dh}, 'h', Nu and 'f' is 4.11%,7.29%,7.85% and 6.16% respectively.
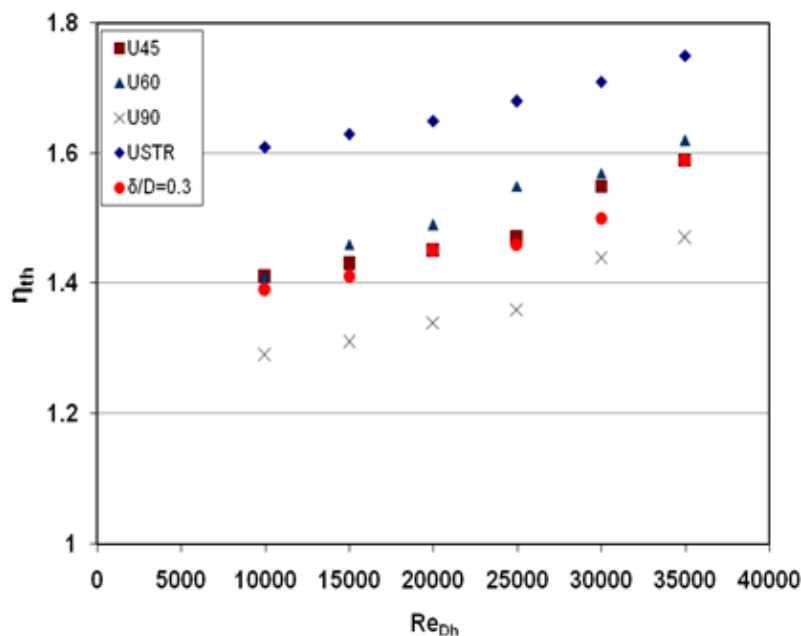
Fig. 12. η_{th} as a function of Re_{Dh} for different arch turbulator

4. Conclusions

The thermal performance and augmented heat transfer rate from the straight arch and curved arch turbulator for dimple depth $\delta/D=0.3$ is presented in this paper. The several salient points emerge from this study as summarized as below

i. Compared to all curved arch turbulator configurations, the thermal performance of 90° curved arch turbulator is lower the dimple depth of 0.3. While thermal performance of 45°and 60° curved and straight arch turbulator is higher than the dimple depth of 0.3. Compared to curved arch, the performance of straight arch turbulator is higher.

ii. The thermal performance of 45°and 60° curved and straight arch turbulator is higher due to top and bottom straight and curved edges breaks the shear layer and force the fluid inside the dimple with higher intercity to reduce low velocity zone and enhance heat transfer.

iii.   The two side legs form the secondary flow, which disturbs the growth of boundary layer before the dimple and enhances the rate of heat transfer within the dimple. As well as increases the intensity of formation of vortices at trailing edge.

iv.   The turbulator provides a very simple but promising compound augmentation technique with moderate pressure penalty.

Acknowledgement

References

[1]   Afanasyev, V. N., Ya P. Chudnovsky, A. I. Leontiev, and P. S. Roganov. "Turbulent flow friction and heat transfer characteristics for spherical cavities on a flat plate." *Experimental Thermal and Fluid Science* 7, no. 1 (1993): 1-8. https://doi.org/10.1016/0894-1777(93)90075-T

[2]   Bunker, Ronald S., and Katherine F. Donnellan. "Heat transfer and friction factors for flows inside circular tubes with concavity surfaces." *Journal of Turbomachinery* 125, no. 4 (2003): 665-672. https://doi.org/10.1115/1.1622713

[3]   Ligrani, Phil M., Mauro M. Oliveira, and Tim Blaskovich. "Comparison of heat transfer augmentation techniques." *AIAA Journal* 41, no. 3 (2003): 337-362. https://doi.org/10.2514/2.1964

[4]   Syred, Nicholas, A. Khalatov, A. Kozlov, A. Shchukin, and R. Agachev. "Effect of surface curvature on heat transfer and hydrodynamics within a single hemispherical dimple." *Journal of Turbomachinery* 123, no. 3 (2001): 609-613. https://doi.org/10.1115/1.1348020

[5]   Chyu, M. K., Y. Yu, H. Ding, J. P. Downs, and F. O. Soechting. *Concavity enhanced heat transfer in an internal cooling passage*. Vol. 78705. American Society of Mechanical Engineers, 1997. https://doi.org/10.1115/97-GT-437

[6]   Moon, H. K., T. O'connell, and B. Glezer. "Channel height effect on heat transfer and friction in a dimpled passage." *Journal of Engineering for Gas Turbines and Power* 122, no. 2 (2000): 307-313. https://doi.org/10.1115/1.483208

[7]   Mahmood, G. I., M. L. Hill, D. L. Nelson, P. M. Ligrani, H-K. Moon, and B. Glezer. "Local heat transfer and flow structure on and above a dimpled surface in a channel." *Journal of Turbomachinery* 123, no. 1 (2001): 115-123. https://doi.org/10.1115/1.1333694

[8]   Isaev, Sergey Aleksandrovich, A. I. Leontiev, Nikolai Anatol'evich Kudryavtsev, and I. A. Pyshnyi. "The effect of rearrangement of the vortex structure on heat transfer under conditions of increasing depth of a spherical dimple on the wall of a narrow channel." *High Temperature* 41, no. 2 (2003): 229-232.

[9]   Ligrani, P. M., G. I. Mahmood, J. L. Harrison, C. M. Clayton, and D. L. Nelson. "Flow structure and local Nusselt number variations in a channel with dimples and protrusions on opposite walls." *International Journal of Heat and Mass Transfer* 44, no. 23 (2001): 4413-4425. https://doi.org/10.1016/S0017-9310(01)00101-6

[10]   Patil, Adhikrao S., Sandeep S. Kore, and Narayan K. Sane. "Experimental investigation of the effect of flow blockages on heat transfer and fluid friction in a round tube using wall-attached circular rings." *Heat Transfer Research* 50, no. 1 (2019). https://doi.org/10.1615/HeatTransRes.2018025424

[11]   Yadav, Rupesh J., Sandeep S. Kore, and Prathamesh S. Joshi. "Correlations for heat transfer coefficient and friction factor for turbulent flow of air through square and hexagonal ducts with twisted tape insert." *Heat and Mass Transfer* 54, no. 5 (2018): 1467-1475. https://doi.org/10.1007/s00231-017-2241-y

[12]   Yadav, Rupesh J., Tejas Mahajani, Sandeep S. Kore, Prakash M. Gadhe, and Dhanpal A. Kamble. "Investigation of heat transfer characteristics using Fe_3O_4 nanofluid along with TT inserts in tube with uniform electromagnetic field." *Applied Nanoscience* 13, no. 1 (2023): 763-785. https://doi.org/10.1007/s13204-021-01905-5

[13]   Waware, Shital Yashwant, Sandeep Sadashiv Kore, and Suhas Prakashrao Patil. "Heat Transfer Enhancement in Tubular Heat Exchanger with Jet Impingement: A Review." *Journal of Advanced Research in Fluid Mechanics and Thermal Sciences* 101, no. 2 (2023): 8-25. https://doi.org/10.37934/arfmts.101.2.825

[14]   Kore, Sandeep Sadashiv, Manoj Kumar Chaudhary, Adhikrao Sarjerao Patil, and Vijay Dilip Kolate. "Computational study and enhancement of heat transfer rate by using inserts introduced in a heat exchanger." *Journal of Advanced Research in Fluid Mechanics and Thermal Sciences* 103, no. 1 (2023): 16-29. https://doi.org/10.37934/arfmts.103.1.1629

[15]   Patankar, Suhas. *Numerical heat transfer and fluid flow*. CRC Press, 1980.

[16]   Kline, Stephen J., and F. A. McClintock. "Describing uncertainties in single-sample experiments." *Mechanical Engineering* 75 (1963): 3-8.

[17]   Miller R. W. *Flow measurement engineering handbook. 2nd Ed*. McGraw-Hill, 1989.